H3K4 Methylation Dependent and Independent Chromatin Regulation by *JHD2* and *SET1* in Budding Yeast

Kwan Yin Lee, Ziyan Chen, River Jiang, and Marc D. Meneghini[1]
Department of Molecular Genetics, University of Toronto, ON M5G 1M1, Canada

ABSTRACT Set1 and Jhd2 regulate the methylation state of histone H3 lysine-4 (H3K4me) through their opposing methyltransferase and demethylase activities in the budding yeast *Saccharomyces cerevisiae*. H3K4me associates with actively transcribed genes and, like both *SET1* and *JHD2* themselves, is known to regulate gene expression diversely. It remains unclear, however, if Set1 and Jhd2 act solely through H3K4me. Relevantly, Set1 methylates lysine residues in the kinetochore protein Dam1 while genetic studies of the *S. pombe SET1* ortholog suggest the existence of non-H3K4 Set1 targets relevant to gene regulation. We interrogated genetic interactions of *JHD2* and *SET1* with essential genes involved in varied aspects of the transcription cycle. Our findings implicate *JHD2* in genetic inhibition of the histone chaperone complexes Spt16-Pob3 (FACT) and Spt6-Spn1. This targeted screen also revealed that *JHD2* inhibits the Nrd1-Nab3-Sen1 (NNS) transcription termination complex. We find that while Jhd2's impact on these transcription regulatory complexes likely acts via H3K4me, Set1 governs the roles of FACT and NNS through opposing H3K4-dependent and -independent functions. We also identify diametrically opposing consequences for mutation of H3K4 to alanine or arginine, illuminating that caution must be taken in interpreting histone mutation studies. Unlike FACT and NNS, detailed genetic studies suggest an H3K4me-centric mode of Spt6-Spn1 regulation by *JHD2* and *SET1*. Chromatin immunoprecipitation and transcript quantification experiments show that Jhd2 opposes the positioning of a Spt6-deposited nucleosome near the transcription start site of *SER3*, a Spt6-Spn1 regulated gene, leading to hyper-induction of *SER3*. In addition to confirming and extending an emerging role for Jhd2 in the control of nucleosome occupancy near transcription start sites, our findings suggest some of the chromatin regulatory functions of Set1 are independent of H3K4 methylation.

Methylation of histone H3 lysine-4 (H3K4me) represents one of the most comprehensively studied chromatin modifications. Like most histone lysine methylations, H3K4 exhibits mono, di, and tri-methylated states (H3K4me1, H3K4me2, and H3K4me3) that have distinctive

regulatory outputs reflecting the recruitment of effector proteins (SANTOS-ROSA *et al.* 2003; TAVERNA *et al.* 2006; KIM AND BURATOWSKI 2009). In the budding yeast *Saccharomyces cerevisiae*, H3K4me levels are controlled by the opposing functions of two highly conserved enzymes belonging to the Trithorax/MLL and JARID1 families: the Set1 methyltransferase and the Jhd2 demethylase (KROGAN *et al.* 2002; INGVARSDOTTIR *et al.* 2007; LIANG *et al.* 2007). Unless otherwise stated, whenever we refer to *SET1* and *JHD2*, we are signifying the budding yeast genes specifically. While Jhd2 appears to act alone, Set1, like Trithorax/MLL, functions within COMPASS, a conserved complex of proteins that function in Set1 targeting and regulation (KROGAN *et al.* 2002). Surprisingly, despite the crucial role of Trithorax/MLL and JARID during development and disease in animals, neither *SET1* nor *JHD2* are essential for cell viability in budding yeast (BENEVOLENSKAYA *et al.* 2005; DEY *et al.* 2008; LOPEZ-BIGAS *et al.* 2008). Moreover, *JHD2* null mutants (*jhd2Δ*) have surprisingly limited phenotypic impact in

otherwise wild-type (WT) mitotic cells grown in the presence of glucose, confounding the study of this important chromatin regulatory protein using yeast (LENSTRA *et al.* 2011; XU *et al.* 2012).

Previously, we found that *JHD2* exhibits specific functions during the gametogenesis phase of the budding yeast life cycle, also known as sporulation (XU *et al.* 2012). The formation of robust spores requires that *JHD2* maintain a period of productive transcription in the face of encroaching and developmentally programmed transcriptional quiescence. During this period, *JHD2* globally demethylates H3K4 at intergenic regions upstream of transcription start sites (TSSs) and overlapping with transcription termination sites (TTSs). Associated with these H3K4me defects, *JHD2* also represses the accumulation of noncoding intergenic transcripts genome-wide (XU *et al.* 2012). These findings suggest roles for *JHD2* in diverse aspects of transcription, including those related to termination and its associated mRNA processing pathways. Indeed, a recent study found that Jhd2 physically interacts with CPF (cleavage and polyadenylation factor) and causes defects in mRNA 3′ untranslated region length for some genes (BLAIR *et al.* 2016). More recently, we determined that H3K4 demethylation by Jhd2 occurs not only during sporulation, but also in mitotic cells in response to non-fermentable carbon sources or to nitrogen manipulations that lead to increased levels of alpha-ketoglutarate, an intermediary metabolite essential for demethylase activity of Jhd2 and the entire Jumonji family of demethylases to which JARIDs belong (LIANG *et al.* 2007; SOLOVEYCHIK *et al.* 2016).

Our previous studies identified developmental/nutritional contexts during which *JHD2* impacts gene expression, but the mechanisms remain opaque. To gain further insight into genetic pathways by which *JHD2* and *SET1* impact gene expression, we used a targeted screening approach. Because genome-wide screens have been unsuccessful in the identification of gene deletions that exhibit interactions with *jhd2Δ* ((COSTANZO *et al.* 2016), our unpublished findings), we selected essential components of the transcriptional machinery and tested whether temperature sensitive (TS) mutants of these components genetically interact with *jhd2Δ*, and in most cases, *set1Δ* as well. Using this approach, we find that *JHD2* genetically inhibits the essential RNA PolII transcription regulatory complexes Spt6-Spn1, FACT (facilitates chromatin transcription), and NNS (Nab3-Nrd1-Sen1) (FORMOSA *et al.* 2001; VASILJEVA AND BURATOWSKI 2006; MCDONALD *et al.* 2010). More detailed genetic experiments reveal that *JHD2*'s inhibitory role can be attributed solely to reversal of H3K4me. Accordingly, genetic interrogation of *SET1* confirms a positive regulatory impact of H3K4me, but also illuminates a counterbalancing and inhibitory role of *SET1* that acts independent of H3K4me. Using molecular biological experiments, we determine that Jhd2 opposes the positioning of a Spt6-Spn1-deposited nucleosome near the 3′ of the *SRG1* non-coding transcript, and accordingly impacts the induction of the downstream *SER3* gene known to be regulated by *SRG1*, perhaps explaining at least some of the basis for the genetic interactions. In summary, our findings identify three transcriptional regulatory complexes subject to regulation by Jhd2 and Set1, and illuminate that *SET1* impinges upon them through H3K4me dependent and independent means.

MATERIALS AND METHODS

Yeast Strains and Plasmids

Standard yeast genetic methods were used for construction of all strains. Yeast strains and plasmids used in this study are listed in Table S1. All strains were constructed through genetic crosses followed by dissections the BY4742 background. Yeast strains were inoculated into several mL of YPD (1% yeast extract, 2% peptone, and 2% glucose) and

grown overnight at room temperature (23°). Each strain was diluted to an $OD_{600} = 0.4$, serially diluted five times and spotted on synthetic complete media (YNB media (Multicell Wisent) containing 5 g/L of ammonium sulfate and either 2% glucose or 2% galactose.

Western blots

Exponential cultures with OD_{600} between 1-2 were lysed by vortexing with acid washed glass beads in SUMEB buffer as described previously (Xu *et al.* 2012). Total protein concentration was quantified using an RC/DC assay (BioRad). Equal amounts of protein were electrophoresed on 12% SDS-PAGE gels, and transferred onto Amersham Hybond-P membranes (GE). Immunoblot analysis was performed using standard procedures. All blots were scanned with a ChemiDoc XRS+ Imaging System. Band intensities were quantified using ImageJ 1.51 v software.

Chromatin immunoprecipitation

Strains were grown at 30° in YPD to OD_{600} 0.8. Crosslinking was performed in 1% formaldehyde for 15 min at room temperature (23°) and then immediately quenched with glycine at a final concentration of 125 mM. Cells were pelleted and washed 2 times with ice cold PBS. Cell pellets were snap frozen in 2 mL screwcap tubes using liquid nitrogen and stored at -80°. Frozen pellets were resuspended in lysis buffer (50 mM HEPES pH 7.5, 140 mM NaCl, 1 mM EDTA pH 8.3, 1% Triton X-100, 0.1% NaDOC) without thawing and topped off with glass beads. Cells were lysed through multiple rounds of beadbeating and then sonicated to shear the chromatin to fragment sizes of approximately 200 to 500 bp. Cross-linked chromatin fragments were immunoprecipitated with antibody overnight. Protein A-Sepharose beads were then added to the samples, and samples were incubated for 90 min. The immunoprecipitated complexes were washed with lysis buffer, lysis buffer containing 500 mM NaCl, wash buffer (10 mM Tris-HCl pH 8.0, 0.25M LiCl, 0.5% NP40, 0.5% NaDOC, 1mM EDTA pH 8.3), and TE (10 mM Tris-HCl pH 8.0, 1 mM EDTA). Next, the immunoprecipitated chromatin was eluted from beads with elution buffer (50 mM Tris-HCl pH 8.0, 10 mM EDTA, 1% SDS) and then eluted with TE/0.67% SDS (10 mM Tris-HCl pH 8.0, 1 mM EDTA pH 8.3, 0.67% SDS, 0.334 mg/mL proteinase K). The two elutions were combined. Whole cell extract samples were topped off with TE/1% SDS (10 mM Tris-HCl pH 8.0, 1mM EDTA, pH 8.3, 1% SDS, 0.25 mg/mL proteinase K). Formaldehyde cross-linking was reversed by incubating the eluates at 65° overnight. DNA from the eluates was treated with RNAse A and purified with a QIAquick PCR purification kit (Qiagen). Immunoprecipitated fractions (IP) and whole-cell extracts (Input) containing DNA were analyzed by real-time PCR as described previously (XU *et al.* 2012) using the primers listed in Table S2. SYBR green signal was measured using the BioRad iQ5 Multicolor Real Time PCR Detection System.

SER3 RT-qPCR analysis

5-10 OD equivalents were harvested for RNA extraction. For RT-qPCR, RNA was extracted with acidic phenol at 65° for 30 min. RNA was then purified, precipitated and resuspended in RNAse free water. cDNA was prepared as described previously using random priming (XU *et al.* 2012). Quantitative PCR quantification of cDNA using SYBR green was measured using the BioRad iQ5 Multicolor Real Time PCR Detection System as described previously (XU *et al.* 2012). Primer sequences for *SER3* and *SCR1* are shown in Table S2. Transcript levels for each primer pair tested were normalized to the reference transcript *SCR1*.

SER3 induction assays

Yeast strains were inoculated into several mL of YPD and grown overnight at room temperature (23°). Each strain was diluted to an

$OD_{600} = 0.4$ in synthetic complete media and grown to $OD_{600} = 2$ at 30°. At this time, cells were harvested by centrifugation, washed with water, and resuspended in synthetic media lacking serine. Growth of cells was resumed with constant shaking at 30°. Cell samples were collected at specific intervals and frozen using liquid nitrogen for analysis by RT-qPCR as described previously (XU et al. 2012). Primer sequences for SER3 and SCR1 are shown in Table S2. RNA isolation, cDNA synthesis, and qPCR is described above.

Data availability

The authors state that all data necessary for confirming the conclusions presented in the article are represented fully within the article. Strains are available upon request.

RESULTS

Genetic interactions of JHD2 with essential transcription regulatory factors

We used a targeted screening approach to identify mutants that exhibit genetic interactions with jhd2Δ. Because Jhd2 reverses a histone modification associated with active transcription, we evaluated temperature sensitive (TS) alleles of essential genes related to transcriptional control as interacting candidates of jhd2Δ. We used strains sourced from a library created and curated previously (LI et al. 2011), with the only exceptions being nab3-42 and spt16-319, which we obtained separately (O'DONNELL et al. 2004; DARBY et al. 2012). All strains described here were engineered using genetic crosses and tetrad dissection. Strain fitness was assessed using spot assays to compare growth rates at varied temperatures. Deletion of JHD2 or SET1 did not cause growth defects under these conditions (Figure 1A, B, and C). For all results shown, we isolated at least 2 independently constructed strain replicates through tetrad dissection. Though replicates and WT control strains are not always shown in the interest of space, all results we report here are upheld in these replicates.

Given the physical association of Jhd2 with CPF/CF, we first evaluated jhd2Δ genetic interactions with TS mutations in 10 different subunits of this large complex (BLAIR et al. 2016). Somewhat surprisingly, we failed to identify any reproducible interactions with CPF/CF (Table 1). NNS functions alongside CPF as one of two distinct mRNA processing pathways in budding yeast. Nab3 and Nrd1 encode RRM domain containing proteins that recognize specific sequences in nascent transcripts (STEINMETZ AND BROW 1996; CARROLL et al. 2004; CREAMER et al. 2011). The Sen1 subunit is homologous to the human helicase protein Senataxin and provides the activity that physically dislodges PolII from the DNA (PORRUA AND LIBRI 2013; CHEN et al. 2014). While the majority of mRNA 3′ end processing of protein coding genes occurs through CPF, NNS controls the transcriptional termination and processing of noncoding RNAs. The most widely studied targets of NNS are snRNAs, snoRNAs, and cryptic unstable transcripts (CUTS) (URSIC et al. 1997; STEINMETZ et al. 2001; ARIGO et al. 2006; THIEBAUT et al. 2006).

We found that jhd2Δ robustly suppressed 2 different alleles of NAB3, nab3-42 and nab3-11 (Table 1, Figure 1A and Figure S1A). Deletion of JHD2 also modestly suppressed sen1-1 (Table 1, Figure S1B). As shown, incubation at high temperature was sufficient to eliminate growth of nab3-42, confirming that jhd2Δ did not provide bypass suppression and that Jhd2 therefore acted to inhibit nab3-42 function at semi-permissive temperatures (Figure 1A). Though we only show the lack of bypass suppression for nab3-42 in the interest of space, this was the case with all interactions we report here. NNS termination is coupled with polyadenylation by the TRAMP complex and RNA processing by Exosome (VASILJEVA AND BURATOWSKI 2006; VANACOVA AND STEFL
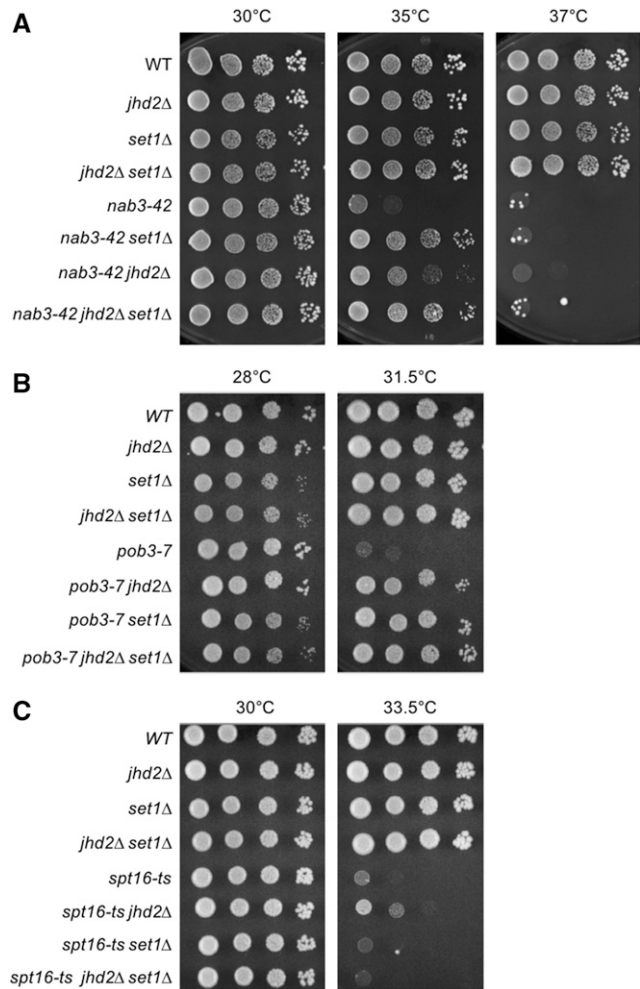

Figure 1 TS alleles of NNS and FACT subunits exhibit genetic interactions with H3K4 modifying enzymes. Yeast strains with the indicated genotypes were serially diluted ten-fold, spotted onto agar plates containing synthetic complete media, and grown at indicated temperatures. Genetic interactions of jhd2Δ and set1Δ with different temperature sensitive alleles of NNS and FACT subunits are shown: (A) nab3-42 (B) pob3-7 (C) spt16-ts.

2007). We observed a similar suppressive interaction of jhd2Δ with the sole essential TRAMP component, MTR4 (Table 1 and data not shown). Interestingly, the only exosome subunit encoding gene we investigated, MTR3, provided the solitary example of a negative interaction with JHD2; jhd2Δ caused a modest but reproducible enhancement of the mtr3-ts growth defect (Table 1 and data not shown).

Among the numerous other essential genes we interrogated, including those contributing to the functions of mediator, RNAPII and its associated C-terminal domain modifications, and TATA binding protein (TBP), only temperature sensitive alleles of genes encoding Spt6-Spn1 and FACT subunits exhibited genetic interactions with jhd2Δ (Table 1, Figure 1B and 1C). Spt6-Spn1 and FACT are conserved heterodimeric histone chaperone complexes that enable RNA PolII transcription through chromatin, deposit nucleosomes in the wake of elongating polymerase, and suppress spurious intragenic transcription (KAPLAN et al. 2003; DUINA 2011; Hainer et al. 2011). While Spt6-Spn1 and FACT have many common and overlapping functions, they exhibit differences in histone binding specificity and in their abilities to disrupt nucleosomes during transcription (BORTVIN AND WINSTON 1996;

Allele	Protein Group	Genetic Interaction
ctf2-1	CPF/CF	N.I.
pti1-ts7	CPF/CF	N.I.
fip1-433	CPF/CF	N.I.
fip1-ph	CPF/CF	N.I.
pap1-1	CPF/CF	N.I.
ssu72-2	CPF/CF	N.I.
clp1-ph	CPF/CF	N.I.
hrp1-7	CPF/CF	N.I.
hrp1-4	CPF/CF	N.I.
rna15-58	CPF/CF	N.I.
rpb2-6	Pol2/CTD	N.I.
rpo21-1	Pol2/CTD	N.I.
rpb3-2	Pol2/CTD	N.I.
rpb5-H147R	Pol2/CTD	N.I.
fcp1-1	Pol2/CTD	N.I.
kin28-ts	Pol2/CTD	N.I.
CTD truncation	Pol2/CTD	N.I.
ess1-H146R	Pol2 CTD isomerase	++
spt15-P65F	TBP	N.I.
mot1-1033	TBP	N.I.
taf5-15	TBP	N.I.
med7-163	Mediator	N.I.
med7-141	Mediator	N.I.
med6-ts	Mediator	N.I.
med4-54	Mediator	N.I.
med4-6	Mediator	N.I.
med8-39	Mediator	N.I.
rox3-182	Mediator	N.I.
nab3-11	NNS	++
nab3-42	NNS	+++
sen1-1	NNS	+
spt6-14	Spt6-Spn1	++
spn1-K192N	Spt6-Spn1	+++
spt16-ts	FACT	+
spt16-319	FACT	+++
pob3-7	FACT	+++
pob3-L78R	FACT	++
mtr4-1	TRAMP	+
mtr3-ts	Exosome	—

Specific TS allele is listed in the left column and the associated protein complex of each factor is shown in the corresponding middle column. In the right column, any observed genetic interactions with *jhd2Δ* are documented. N.I. no interaction, + positive interaction (+ weakest, ++ medium, +++ strong suppression), - weak negative interaction.

ORPHANIDES *et al.* 1999; BELOTSERKOVSKAYA *et al.* 2003; MCCULLOUGH *et al.* 2015). FACT can disrupt and reassemble nucleosomes, while Spt6-Spn1 only has the ability to reassemble them (ORPHANIDES *et al.* 1998; ORPHANIDES *et al.* 1999; BELOTSERKOVSKAYA *et al.* 2003). We also confirmed a previous finding that the temperature sensitive growth defect of *ess1-H146R*, which encodes a CTD-associated prolyl-isomerase, was suppressed by *jhd2Δ* (MA *et al.* 2012).

H3K4me dependent and independent modulation of NNS and FACT by JHD2 and SET1

As *JHD2* reverses H3K4me, we hypothesized that increased H3K4me caused by *jhd2Δ* accounted for the genetic interactions described above. Indeed, H3K4me3 has been suggested to promote NNS function, with *set1Δ* enhancing the growth and termination phenotypes caused by alleles of *NRD1* that delete portions of its N-terminus (TERZI *et al.* 2011).

Terzi *et al.* also showed that *set1Δ* enhanced termination defects caused by *nab3-11*, though they did not evaluate *SET1*'s impact on *nab3-11* growth properties (TERZI *et al.* 2011). We therefore tested if *jhd2Δ* suppression of NNS mutations could occur in the absence of *SET1*. Unexpectedly, *set1Δ* suppressed the growth defect of *nab3-42* to a degree that exceeded *jhd2Δ* suppression, with the triple mutants resembling *nab3-42 set1Δ* (Figure 1A). Terzi *et al.* (2011) found that H3K4me3 promotes NNS function using truncation alleles of *NRD1* (TERZI *et al.* 2011), but the suppression of *nab3-42* by *set1Δ* presented here suggested that H3K4me antagonizes NNS function. To rule out some unusual allele specific interaction of *nab3-42* with *set1Δ*, we replicated the *set1Δ* and *jhd2Δ* interactions with *NAB3* using the *nab3-11* allele (Figure S1A). Furthermore, and consistent with the *NAB3* results, *sen1-1* was also suppressed by both *jhd2Δ* and *set1Δ*, again with the triple mutants resembling *sen1-1 set1Δ* (Figure S1B). While none of our experiments overlap with those of Terzi *et al.*, their findings would not have predicted ours nor vice versa. In particular, our finding that *set1Δ* suppressed the *nab3-11* growth defect is somewhat discordant with Terzi *et al.*'s finding of an aggravating consequence of *set1Δ* on *nab3-11* for transcriptional termination. Among the many possible explanations for this discrepancy, a simple view is that the essential functions of *NAB3* may not be directly reflected by termination defects described by Terzi *et al.*

Our targeted screen also identified the FACT subunit encoding alleles *pob3-7* and *spt16-ts* as exhibiting alleviating genetic interactions with *jhd2Δ* (Table 1, Figure 1B and 1C). Using the same experimental approach as with NNS subunits, we tested if *jhd2Δ* suppression of *pob3-7* and *spt16-ts* required *SET1*. Curiously, and unlike the case with NNS subunits, *pob3-7* and *spt16-ts* exhibited distinct genetic interactions in combination with *set1Δ*, even though both factors function in the FACT complex. We found that *set1Δ* suppressed the growth defect of *pob3-7* mutants to a level comparable to the suppression conferred by *jhd2Δ*, with the triple mutants showing no evidence of synergy (Figure 1B). In contrast, the *spt16-ts* temperature sensitive growth defect was suppressed by *jhd2Δ* in a *SET1* dependent manner, suggesting that H3K4me promotes Spt16 function (Figure 1C). We confirmed these genetic interactions with additional alleles of *POB3* and *SPT16*, *pob3-L78R* and *spt16-319* (Figure S1C and D). The differences in *SET1* genetic interaction phenotypes observed for *SPT16* and *POB3* mutants suggest complexities in nucleosome interactions, or that their encoded proteins may exhibit separable functions apart from the FACT complex.

To investigate how both *set1Δ* and *jhd2Δ* can rescue certain temperature sensitive growth defects, we employed strains that express H3K4 amino acid substitution mutants from a chromosomal locus in place of wild type H3 (DAI *et al.* 2008). The most widely utilized amino acid substitutions for this approach are alanine (H3K4A) and arginine (H3K4R). We first confirmed the histone mutations by sequencing and then determined that H3K4A and H3K4R alone or in combination with *set1Δ* did not cause any growth phenotypes under the conditions of our spotting assays (Figure S2A). Unexpectedly, we found that H3K4A and H3K4R modified *pob3-7* and *nab3-11* mutants in opposing fashion. H3K4A suppressed *pob3-7* and *nab3-11* temperature sensitivity (Figure 2A and Figure S2B). Suppression by H3K4A and *set1Δ* did not display any synergy. H3K4R caused the opposite effect of H3K4A, exacerbating the temperature sensitive growth defect of *nab3-11* and *pob3-7* (Figure 2A, 2B, 2C, Figure S2B, and Figure S3A). We note that this latter result is consistent with previous findings suggesting a positive impact for H3K4me3 on NNS function (TERZI *et al.* 2011).

To shed light on the confounding differences in H3K4A and H3K4R phenotypes, we performed additional studies exploiting an annotated synthetic lethal interaction between *set1Δ* and *csf1Δ* (COSTANZO *et al.* 2016). *CSF1* (cold sensitive for fermentation) encodes a conserved yet

poorly characterized protein required for growth on glucose at low temperatures and is involved in secretory protein maturation and amino acid metabolism. (TOKAI *et al.* 2000; COPIC *et al.* 2009; COSTANZO *et al.* 2016). In support of the interpretation that *csf1Δ set1Δ* lethality was caused by loss of H3K4me, we found that *jhd2Δ* suppressed *csf1Δ* and that *JHD2* overexpression using an integrated galactose-inducible allele enhanced *csf1Δ* (Figure S2C and D). The *csf1Δ* enhancement by *GAL-JHD2* was abrogated by mutation of histidine-427 to alanine (H427A), which renders Jhd2 catalytically inactive (INGVARSDOTTIR *et al.* 2007; LIANG *et al.* 2007) (Figure S2C and D).

We constructed diploid strains heterozygous for *csf1Δ*, *set1Δ*, and H3K4A or H3K4R mutants and interrogated them using tetrad dissections. In addition to confirming *csf1Δ set1Δ* synthetic lethality, we found that H3K4R exhibited synthetic lethality with *csf1Δ* (Figure 2D). In stark contrast, H3K4A had no consequence for *csf1Δ* viability, and remarkably, suppressed the synthetic lethality of *csf1Δ set1Δ* (Figure 2D). We dissected dozens of tetrads and confirmed that this pattern of inheritance was highly stereotypical and not due to random spore inviability (Table 2). It is noteworthy that while both H3K4A and H3K4R abolish H3K4 methylation, arginine retains the positively charged characteristic of lysine
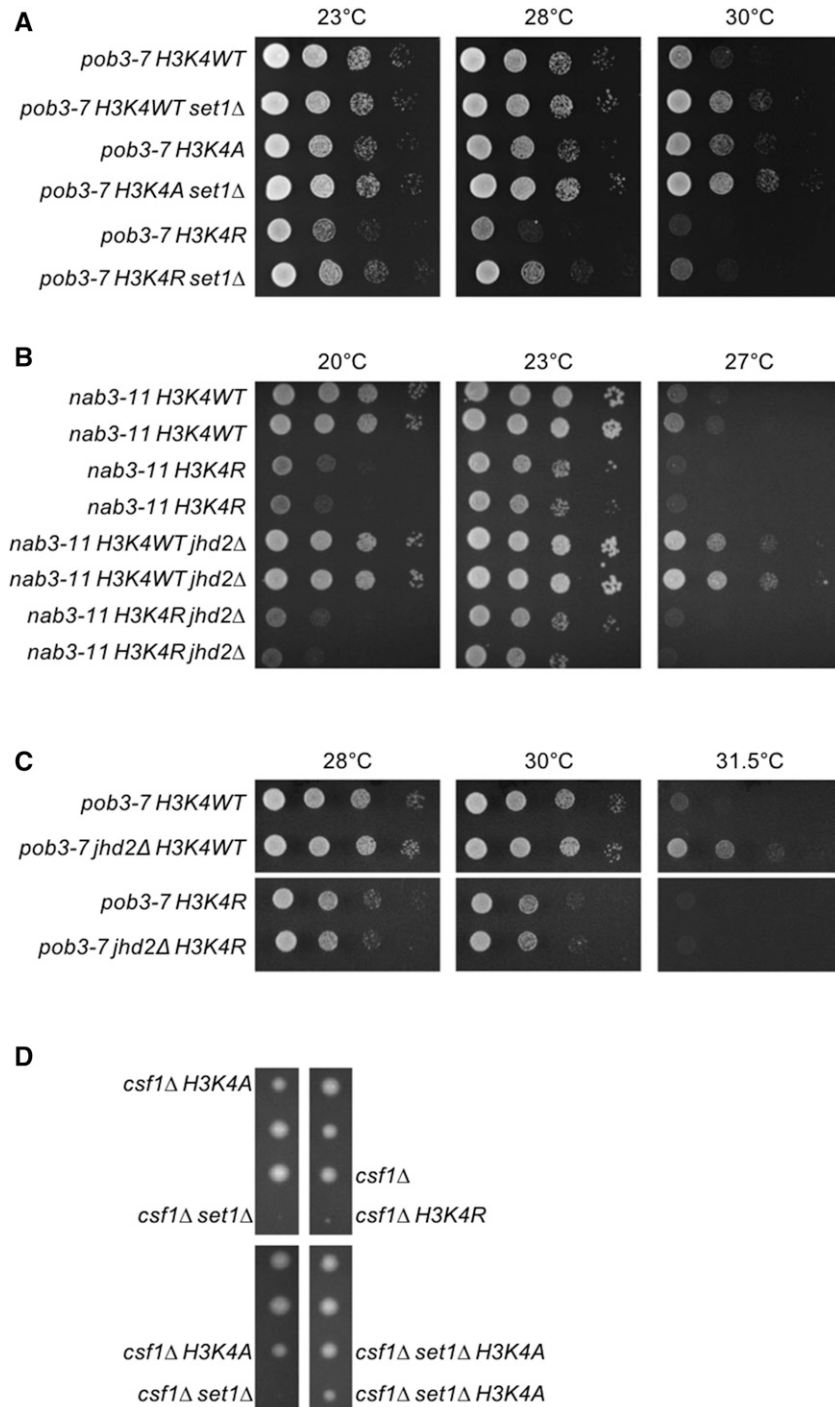

Figure 2 Genetic suppression of NNS and FACT by *set1Δ* and *jhd2Δ* dependent and independent of H3K4me. Plate spot assays (as described in Figure 1) were used to compare the growth of the indicated strains. Isogenic strains were constructed through genetic crosses with H3K4A and H3K4R substitution mutants from the Dharmacon Non Essential Histone H3 & H4 Mutant Collection. (A) Genetic interactions of *set1Δ*, H3K4A, and H3K4R with *pob3-7*. (B) Genetic interactions of *jhd2Δ* and H3K4R with *nab3-11*. Growth of two independent isolates of each genotype is shown. (C) Genetic interactions of *jhd2Δ* and H3K4R with *pob3-7*. (D) Diploid strains containing *csf1Δ*, *set1Δ*, and either H3K4A or H3K4R were sporulated and dissected onto YPD medium. A representative field of the haploid ascospores recovered and their respective genotypes are shown.

in contrast to the aliphatic alanine residue. Accordingly, arginine much more closely resembles the structure of a lysine residue compared with alanine. These results suggest that H3K4R more reliably recapitulates the consequences of set1Δ for chromatin structure and point toward neomorphic characteristics of H3K4A, which seem likely to manifest differently depending on genetic context. We therefore proceeded with our studies using the H3K4R mutant.

To reconcile the H3K4R mutant phenotype with suppression of NNS and FACT subunits by set1Δ, we constructed strains combining H3K4WT or H3K4R with set1Δ and NNS/FACT mutants. We found that set1Δ conferred suppression of the growth phenotypes of pob3-7, nab3-11, and sen1-1 even in the context of H3K4R albeit not to the extent seen in H3K4WT (Figure 2A, Figure S2B, Figure S3A, and B). Thus, the suppression of NNS and FACT subunits by set1Δ in H3K4R mutants suggests that some activity of Set1 acted in opposition to NNS and FACT independent of H3K4me (Figure 3).

To further evaluate the positive impact of H3K4me on NNS and FACT and the role of JHD2 in this, we performed analogous experiments with jhd2Δ. Suppression of nab3-11, pob3-7, and sen1-1 by jhd2Δ could no longer occur in the context of H3K4R, arguing that Jhd2 opposed NNS and FACT function solely through reversal of H3K4me (Figure 2B, 2C, and Figure S3C). Based on these results as well as previous findings from Terzi et al., we propose counterbalancing regulation of NNS and FACT by Set1 and Jhd2, with H3K4me promoting their functions and an unknown inhibitory impact conferred by Set1 in a H3K4 independent manner (Figure 3).

To gain insight into how Set1 opposed FACT independent of H3K4, we constructed strains that had the endogenous SET1 locus replaced with SET1-G951S, an allele that abolishes Set1 enzymatic activity, but does not disrupt the integrity of COMPASS (NAGY et al. 2002; SCHIBLER et al. 2016). We found that SET1-G951S suppressed pob3-7 to an extent that was equivalent to set1Δ in strains expressing a WT allele of H3K4 (Figure S4). As enzymatically dead alleles of SET1 lead to a depletion of Set1 protein levels, this was to be expected (SOARES et al. 2014). Curiously, in strains expressing H3K4R, which do not deplete Set1 levels to nearly the extent seen with enzymatically dead alleles of Set1 (SOARES et al. 2014), SET1-G951S failed to suppress pob3-7 at 30°, but did suppress equivalently to set1Δ at the more stringent temperature of 31.5° (Figure S4). Similar results were obtained with nab3-11 (data not shown). These results, while complex, suggest that the H3K4-independent inhibition of pob3-7 by Set1 may involve both enzymatic and non-enzymatic roles of this protein (Figure 3).

Spt6-Spn1 was opposingly governed by JHD2 and SET1 through H3K4me3

The complexity of interactions exhibited by NNS and FACT with SET1 rendered them difficult to further study without a more detailed understanding of what regulatory functions SET1 has independent of

H3K4. We therefore extended our genetic analysis to Spt6-Spn1. As mentioned above, we determined that TS alleles of both Spt6-Spn1 subunits, spt6-14 and spn1-K192N, were suppressed by jhd2Δ (Table 1, Figure 4A and 4B). In contrast to NNS and FACT, the temperature sensitive growth defects of both Spt6-Spn1 subunits were suppressed by jhd2Δ in a SET1 and H3K4 methylation dependent manner (Figure 4A, B, C, and data not shown). Moreover, and consistent with the interpretation that SET1-mediated H3K4me promoted Spt6-Spn1 function, both set1Δ and H3K4R enhanced the growth defects of spt6-14 and spn1-K192N (Figure 4A, B, C, and data not shown).

To validate that Jhd2 demethylation of H3K4 opposed Spt6-Spn1, we complemented the jhd2Δ-suppressed strains with previously described JHD2 expressing plasmids (MERSMAN et al. 2009). Cells harboring these plasmids express JHD2 under the control of a constitutive PYK1 promoter, which leads to modestly increased levels of Jhd2 and associated decreased H3K4me3 levels. These effects on H3K4me could be abrogated by the H427A mutation or by deletion of its conserved PHD domain, which may enable Jhd2 recruitment to chromatin (MERSMAN et al. 2009). As expected, we found that jhd2Δ suppression of spt6-14 and spn1-K192N could be reverted by JHD2 complementation and that the growth defects of spt6-14 and spn1-K192N were in fact enhanced by the JHD2 overexpressing plasmids (Figure S5A and B). Importantly, this suppression was lost in the H427A and PHD domain mutants (which both encode stable proteins (MERSMAN et al. 2009)) (Figure S5A and B). Our findings support the conclusion that suppression of Spt6-Spn1 alleles by jhd2Δ was due to the loss of H3K4 demethylation.

To gain insights into which H3K4 methylation species accounted for suppression of Spt6-Spn1, we genetically interrogated COMPASS complex subunits known to specifically perturb H3K4me3 or H3K4me3 and -me2. The effects of bre2Δ and spp1Δ on H3K4me have been extensively described. Deletion of BRE2 results in a complete loss of H3K4me3 and a significant decrease of H3K4me2 but no change in H3K4me1, while spp1Δ results in a substantial decrease of H3K4me3 with no detectable consequence on bulk H3K4me2 or -me1 (SCHNEIDER et al. 2005; DEHÉ et al. 2006; TAKAHASHI et al. 2009; MARGARITIS et al. 2012). As with set1Δ, we found that both bre2Δ and spp1Δ enhanced the growth defect of spn1-K192N (Figure 4D). Moreover, jhd2Δ suppression of spn1-K192N was completely dependent on BRE2 and SPP1 (Figure 4D). We compared bulk H3K4me3 levels by western blot in spt6-14 and spt6-14 jhd2Δ at a semi-permissive temperature. Consistent with the genetic data, we observed a modest increase in bulk H3K4me3 levels in the spt6-14 jhd2Δ double mutant (Figure 4E). We confirmed the reproducibility of this by quantifying the relative abundance of H3K4me3/H3 as well as of H3/Pgk1 from three biological replicates of spt6-14 and spt6-14 jhd2Δ (Figure S6). Collectively, our data support the conclusion that JHD2 and SET1 opposingly governed the function of Spt6-Spn1 through H3K4me3 (Figure 3).

■ Table 2 Observed and expected genetic frequencies of csf1Δ with histone H3K4A and H3K4R amino acid substitution mutants

	H3K4			
Genotype	WT	A	R	Expected frequency
csf1Δ	12 (0.16)	7 (0.09)	0 (0.00)	0.125
set1Δ csf1Δ	0 (0.00)	9 (0.11)	0 (0.00)	0.125
Total number of spores	73	79	71	

Diploid strains mmy7658 (H3K4R), mmy7659 (H3K4WT), and mmy7660 (H3K4A) were sporulated and dissected onto YPD medium. These strains are heterozygous for set1Δ, csf1Δ, and the corresponding histone amino acid substitution. The observed frequency of each genotype was calculated by dividing to the total number of spores counted and is shown in the parentheses.
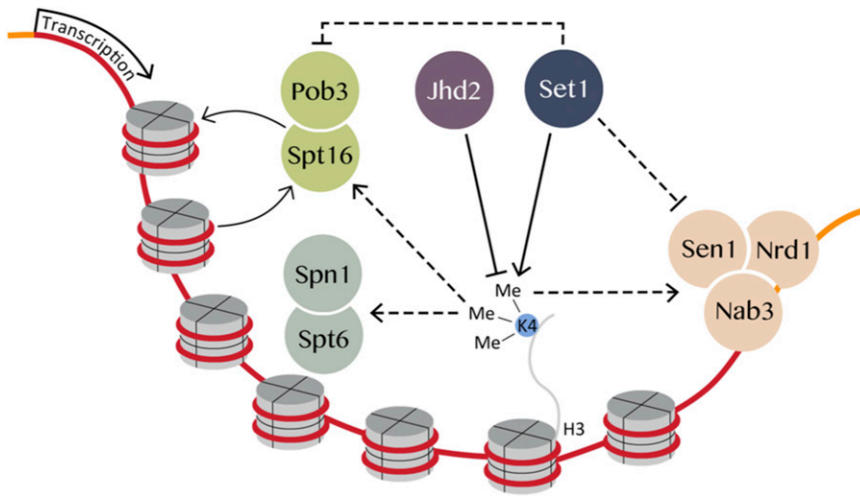
Figure 3 Genetic model of FACT and NNS regulation by Set1 and Jhd2. Methylation of H3K4 promoted FACT and NNS function while Set1 exhibited an inhibitory function independent of H3K4. Spt6-Spn1 is positively regulated by H3K4me3.

JHD2 repressed TSS-associated nucleosome occupancy and transcriptional induction of a Spt6-Spn1 regulated gene

Reflecting its role in the recycling of nucleosomes in the wake of elongating PolII, Spt6-Spn1 mutation causes reduced histone occupancy genome-wide (IVANOVSKA *et al.* 2011). We asked if *jhd2Δ* suppression of Spt6-Spn1 involved a reversal of these histone occupancy defects. First, we used western blots to measure bulk histone H3 levels and found that *jhd2Δ*, *set1Δ*, and *spt6-14* mutants showed no apparent defects in histone H3 levels at the permissive temperature of 23° (Figure 5A).
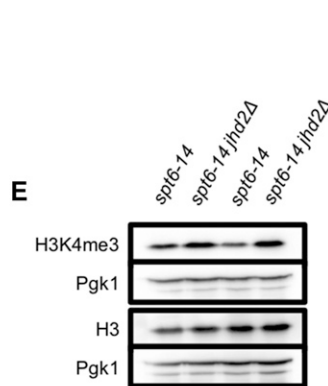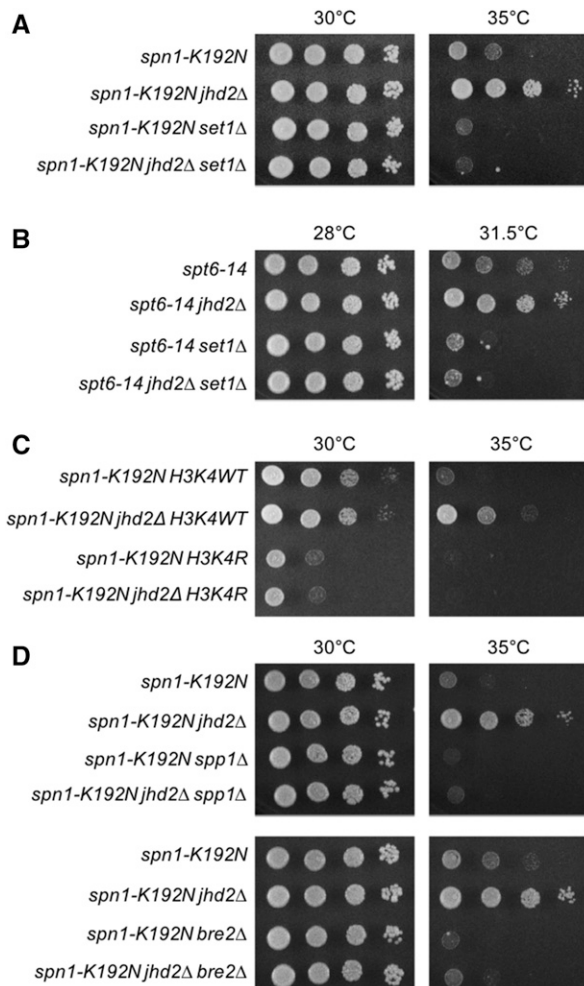

Figure 4 Spt6-Spn1 complex temperature sensitive mutants are rescued by an increase in H3K4me3 through *jhd2Δ*. Plate spot assays (as described in Figure 1) were used to compare the growth of the indicated strains. Genetic interactions of *jhd2Δ* and *set1Δ* with Spt6-Spn1 are shown: (A) *spt6-14* (B) *spn1-K192N*. (C) Isogenic strains were constructed through genetic crosses with the H3K4R substitution mutant from the Dharmacon Non Essential Histone H3 & H4 Mutant Collection. Genetic interactions of *jhd2Δ* and H3K4R with *spn1-K192N*. (D) Genetic interactions of *jhd2Δ*, nonessential COMPASS subunits *spp1Δ* and *bre2Δ*, and *spn1-K192N*. (E) Western blot analysis of H3K4me3, Histone H3, and Pgk1 were performed on biological duplicates of *spt6-14* and *spt6-14 jhd2Δ* grown at 30°C. Pgk1 serves as a loading control.

At the semi-permissive temperature of 30° *spt6-14* exhibited a dramatic reduction in H3 levels, consistent with its role as a histone chaperone (Figure 5A). This reduction was not reversed by *jhd2Δ* suggesting that suppression did not occur by generically improving Spt6-Spn1 histone recycling or chaperone function (Figure 4E, 5A, and Figure S6).

To gain more detailed insight into the relationship between Jhd2 and Spt6-Spn1, we measured chromatin-associated histone H3 in WT, *jhd2Δ*, *spt6-14*, and *spt6-14 jhd2Δ* cells at the *SRG1-SER3* locus using chromatin immunoprecipitation with an anti-H3 antibody followed by real time PCR quantification of the immunoprecipitated DNA (ChIP-qPCR). In order to evaluate nucleosome positions at high resolution across *SRG1-SER3*, we used 33 closely spaced PCR amplicons to measure immunoprecipitated DNA (Hainer *et al.* 2011). The averaged results of 3 independent biological experiments are shown (Figure 5B). As previously described, an abundance of H3 was detected throughout the *SRG1* transcript unit extending into the *SER3* gene in

WT cells. These H3 levels were dramatically depleted in *spt6-14* mutants grown at the semi-permissive temperature (30°C), confirming that their deposition was Spt6 dependent (Hainer *et al.* 2011) (Figure 5B). Consistent with our western blotting results, *spt6-14 jhd2Δ* mutants did not exhibit improved H3 deposition at *SRG1-SER3* at the semi-permissive temperature we used (Figure 5B). In WT and *jhd2Δ* cells with normal *SPT6* function, the H3 ChIP profiles were nearly superimposable throughout the entire *SRG1-SER3* region with one conspicuous exception: *jhd2Δ* caused a highly significant increase in H3 abundance at a single distinctive peak near the 3′ end of the *SRG1* transcript unit, presumably reflecting a well-positioned nucleosome (Figure 5B, peak denoted with a red asterisk, $P < 0.05$). This *JHD2*-repressed nucleosome was positioned ∼75 base pairs upstream of the *SER3* TSS, and positioned ∼75 base pairs downstream of this TSS we observed an additional H3 ChIP peak in *jhd2Δ*, though this second peak was not statistically significant (Figure 5B, denoted with a blue arrow). Spanning the *SER3* TSS, H3 ChIP signal was noisy in both WT
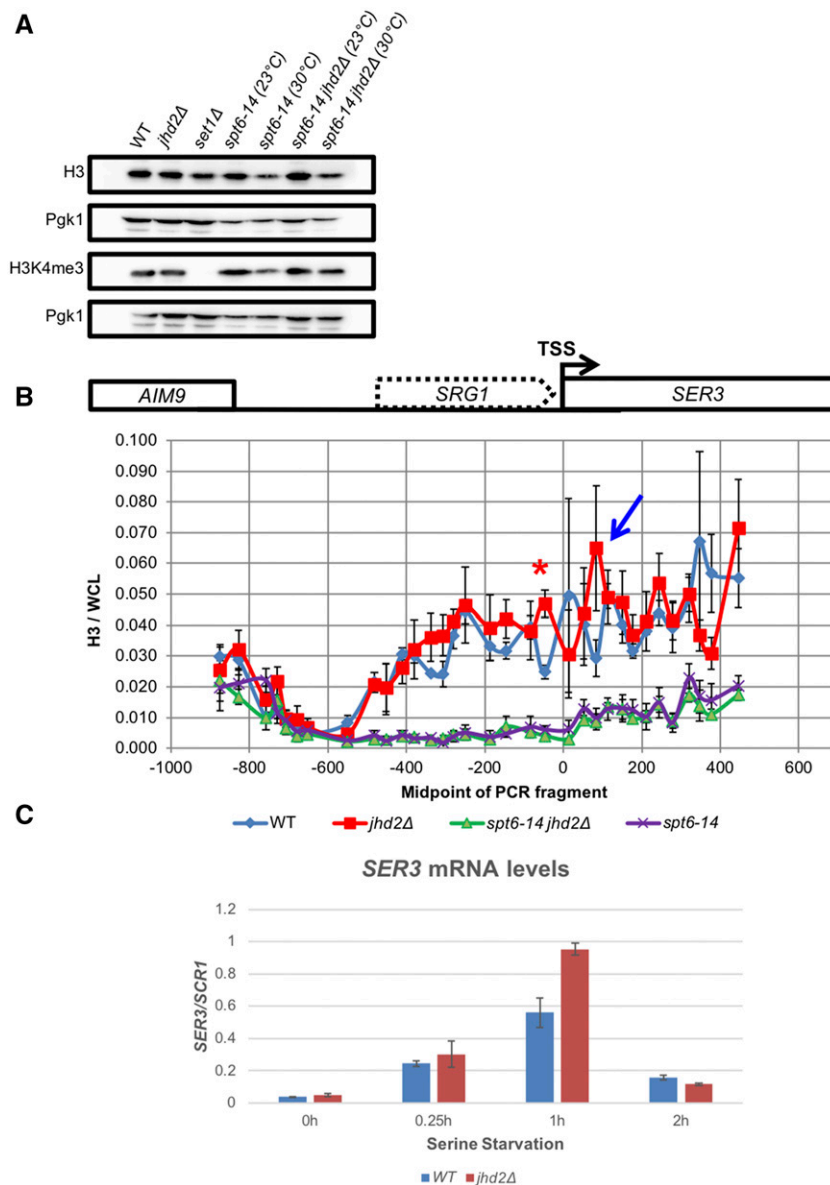

Figure 5 *JHD2* deletion does not rescue Spt6-Spn1 mutants by compensating for defects in chromatin structure. (A) Western blot detection of H3K4me3, pan-H3, and Pgk1 are shown from extracts of wild-type and mutant cells grown at 23°C (permissive) and 30°C (semi-permissive temperature). Pgk1 serves as a loading control. (B) Histone H3 ChIP was performed on strains grown at 30°C (semi-permissive temperature) across the *SRG1-SER3* locus (schematic of locus shown above graph). H3 ChIP signal was normalized to signal from whole cell lysate (WCL) DNA. The transcription start site of *SER3* is positioned at 0 and for *SRG1* at -480. Error bars represent standard error of the mean. Significance as calculated by a two-tailed student's *t*-test is shown where *$P < 0.05$. A blue arrow denotes an additional H3 ChIP peak in *jhd2Δ* that was not statistically significant. (C) *SER3* transcript level was measured by RT-qPCR at specific intervals after serine withdrawal in wildtype and *jhd2Δ* mutants. *SER3* signal was normalized to *SCR1*.

and *jhd2Δ*, suggesting a dynamic state of nucleosomal occupancy at this region (Figure 5B).

We performed our ChIP experiments from cells grown in rich media, a condition in which *SER3* transcription is repressed in a manner dependent on Spt6-Spn1-deposited nucleosomes across the *SER3* TSS in response to *SRG1* transcription (PRUNESKI AND MARTENS 2011) (Figure 5B). A simple encapsulation of our findings posits that *JHD2* prevented Spt6-Spn1-deposited nucleosomes from accumulating at positions on the flanks of the *SER3* TSS, resulting in dynamic and noisy nucleosome occupancy across the *SER3* TSS (Figure 5B). We detected no differences in *SER3* abundance from WT and *jhd2Δ* cells grown in rich media, suggesting that this altered chromatin architecture did not impact *SER3* repression (data not shown). To determine if it instead impacted *SER3* induction, we subjected WT and *jhd2Δ* cells to serine starvation and compared their relative *SER3* mRNA abundance using quantitative PCR amplification of reverse transcribed RNA (RT-qPCR). We found that *SER3* was maximally expressed 1 hr after serine withdrawal, and that *SER3* mRNA accumulated to ∼1.7 increased levels in *jhd2Δ* at this timepoint (Figure 5C). Following 2 hr of serine starvation, yeast cells adapt and repress *SER3* induction, and *jhd2Δ* had no consequence for this repression (MARTENS *et al.* 2005) (Figure 5C). Thus, the phased nucleosomes flanking the *SER3* TSS we observed in *jhd2Δ* were associated with a hyper-induction of *SER3*.

DISCUSSION

In this work, we identify novel genetic interactions between the H3K4 demethylase *JHD2* and genes encoding subunits of the essential transcription regulatory complexes NNS, FACT, and Spt6-Spn1. Our genetic findings support the conclusion that reversal of H3K4me by Jhd2 opposes the functions of these complexes (Figure 3). In the case of NNS, our findings are in good agreement with a previous study suggesting that H3K4me3 promotes NNS function (TERZI *et al.* 2011). A simple prediction from our findings is that *set1Δ*, which abolishes all H3K4 methylation, should cause the opposite phenotype as, and exhibit epistasis to, *jhd2Δ*. While this was indeed the case for Spt6-Spn1 and the *SPT16* subunit of FACT, TS alleles of *SEN1*, *NAB3*, and *POB3* were each suppressed by *set1Δ* to an extent equivalent to, or exceeding that by *jhd2Δ*. More detailed genetic studies revealed that *SET1* opposed the functions of *SEN1*, *NAB3*, and *POB3* in a manner that was independent of H3K4me. We point out that the Swd2 subunit of COMPASS also functions within the NNS-related termination complex APT, which could potentially explain the different NNS interactions with *SET1* deletion *vs.* K4 mutation shown in this study (Nedea *et al.* 2003; Soares and Buratowski 2012). Our genetic model posits that H3K4me positively influences NNS and FACT functions, and that Set1 exhibits an additional counterbalancing H3K4me-independent activity that negatively impacts these complexes (Figure 3). For Spt6-Spn1, our genetic data suggested a positive impact by H3K4me3 with no repressive H3K4-indpendent role for Set1 (Figure 3). Our molecular studies showed that Jhd2, and by inference H3K4me reversal, negatively regulated the accumulation of Spt6-Spn1 deposited nucleosomes flanking the *SER3* TSS, resulting in hyper-induction of *SER3* upon serine starvation.

In contrast to our findings and what has been reported previously (Hainer *et al.* 2011), Ramakrishnan *et al.* found that both *jhd2Δ* and *set1Δ* caused dramatic down-regulation of *SER3* in rich serine-replete conditions (RAMAKRISHNAN *et al.* 2016). Under such conditions *SER3* is normally strongly repressed, and we found that levels were so low as to be nearly undetectable with no difference between WT and *jhd2Δ* (Figure 5C) (MARTENS *et al.* 2004; MARTENS *et al.* 2005; Hainer *et al.* 2011). To reconcile these discrepancies, we point out that all of the

experiments in the Ramakrishnan *et al.* study were performed in a strain background that utilized plasmid expressed histone H2A-H2B, with the endogenous H2A-H2B genes deleted, a condition known to reduce histone dosage and alter transcription (CLARK-ADAMS *et al.* 1988). This is not to say we reject the findings of Ramakrishnan *et al.*; rather, the findings of Ramakrishnan *et al.* seem to illuminate a facile way to investigate chromatin biology in yeast, by 'sensitizing' the chromatin through reduced histone dosage. Whatever the case may be, our findings uphold an emerging role for Jhd2 in the control of nucleosome occupancy at TSS's and TTS's. *JHD2*'s known developmental role in opposing nucleosome accumulation at these regions may be attributable to it antagonistic impact on Spt6-Spn1 (XU *et al.* 2012). As Spt6-Spn1, Set1, Jhd2, and H3K4me are conserved throughout eukaryotes, these mechanisms may have broad significance.

An important feature of our findings relates to functions of Set1 that are independent H3K4 methylation. The only confirmed non-H3K4 enzymatic target of Set1, or indeed of any member of this highly conserved family of enzymes, is the essential kinetochore protein Dam1. Dam1 lysine residue methylation by Set1 regulates the phosphorylation status of neighboring serine residues by mediating the opposing activities of Ipl1 and Glc7 kinase and phosphatase (ZHANG *et al.* 2005). *Schizosaccharomyces pombe* Set1 (_sp_Set1) controls transcription at silent mating loci, telomeric regions, and retrotransposon (Tf) elements, as well as the clustering of diverse genomic regions encoding Tf elements. Interestingly, _sp_Set1 accomplishes these sundry functions in a manner dependent on differing domains of Set1 that do, or do not, have consequences for H3K4me. The two key regulatory roles of _sp_Set1 appear dependent on _sp_Set1's enzymatic activity and on its RNA binding RRM2 domain, a domain found in both fission and budding yeast Set1 (Trésaugues *et al.* 2006; LORENZ *et al.* 2014; MIKHEYEVA *et al.* 2014). Consistent with the RRM2 having important regulatory significance independent of H3K4me, a recent study identified many mRNA targets bound by the budding yeast Set1 RRM2 domain (SAYOU *et al.* 2017). Thus, the RRM2 domain may underlie at least some of the H3K4me-independent regulatory functions of Set1 we identify here. Our genetic results, however, also suggest that enzymatic activity of Set1 directed toward a non-H3K4 substrate has regulatory significance, as may be the case for *S. pombe* Set1 (LORENZ *et al.* 2014; MIKHEYEVA *et al.* 2014). It seems highly plausible that chromatin-associated factors may be targets of regulatory lysine methylation by Set1 and other histone methyltransferases.

LITERATURE CITED

Arigo, J. T., D. E. Eyler, K. L. Carroll, and J. L. Corden, 2006   Termination of cryptic unstable transcripts is directed by yeast RNA-binding proteins Nrd1 and Nab3. Mol. Cell 23(6): 841–851. https://doi.org/10.1016/j.molcel.2006.07.024

Belotserkovskaya, R., S. Oh, V. A. Bondarenko, G. Orphanides, V. M. Studitsky *et al.*, 2003   FACT facilitates transcription-dependent nucleosome alteration. Science 301(5636): 1090–1093. https://doi.org/10.1126/science.1085703

Benevolenskaya, E. V., H. L. Murray, P. Branton, R. A. Young, and W. G. Kaelin, Jr., 2005   Binding of pRB to the PHD protein RBP2 promotes cellular differentiation. Mol. Cell 18(6): 623–635. https://doi.org/10.1016/j.molcel.2005.05.012

Blair, L. P., Z. Liu, R. L. Labitigan, L. Wu, D. Zheng et al., 2016   KDM5 lysine demethylases are involved in maintenance of 3′UTR length. Sci. Adv. 2(11): e1501662. https://doi.org/10.1126/sciadv.1501662

Bortvin, A., and F. Winston, 1996   Evidence that Spt6p controls chromatin structure by a direct interaction with histones. Science 272(5267): 1473–1476. https://doi.org/10.1126/science.272.5267.1473

Carroll, K. L., D. A. Pradhan, J. A. Granek, N. D. Clarke, and J. L. Corden, 2004   Identification of cis elements directing termination of yeast non-polyadenylated snoRNA transcripts. Mol. Cell. Biol. 24(14): 6241–6252. https://doi.org/10.1128/MCB.24.14.6241-6252.2004

Chen, X., U. Muller, K. E. Sundling, and D. A. Brow, 2014   Saccharomyces cerevisiae Sen1 as a model for the study of mutations in human Senataxin that elicit cerebellar ataxia. Genetics 198(2): 577–590. https://doi.org/10.1534/genetics.114.167585

Clark-Adams, C. D., D. Norris, M. A. Osley, J. S. Fassler, and F. Winston, 1988   Changes in histone gene dosage alter transcription in yeast. Genes Dev. 2(2): 150–159. https://doi.org/10.1101/gad.2.2.150

Copic, A., M. Dorrington, S. Pagant, J. Barry, M. C. Lee et al., 2009   Genomewide analysis reveals novel pathways affecting endoplasmic reticulum homeostasis, protein modification and quality control. Genetics 182(3): 757–769. https://doi.org/10.1534/genetics.109.101105

Costanzo, M., B. VanderSluis, E. N. Koch, A. Baryshnikova, C. Pons et al., 2016   A global genetic interaction network maps a wiring diagram of cellular function. Science 353: aaf1420.

Creamer, T. J., M. M. Darby, N. Jamonnak, P. Schaughency, H. Hao et al., 2011   Transcriptome-wide binding sites for components of the Saccharomyces cerevisiae non-poly(A) termination pathway: Nrd1, Nab3, and Sen1. PLoS Genet. 7(10): e1002329. https://doi.org/10.1371/journal.pgen.1002329

Dai, J., E. M. Hyland, D. S. Yuan, H. Huang, J. S. Bader et al., 2008   Probing nucleosome function: a highly versatile library of synthetic histone H3 and H4 mutants. Cell 134(6): 1066–1078. https://doi.org/10.1016/j.cell.2008.07.019

Darby, M. M., L. Serebreni, X. Pan, J. D. Boeke, and J. L. Corden, 2012   The Saccharomyces cerevisiae Nrd1-Nab3 transcription termination pathway acts in opposition to Ras signaling and mediates response to nutrient depletion. Mol. Cell. Biol. 32(10): 1762–1775. https://doi.org/10.1128/MCB.00050-12

Dehé, P. M., B. Dichtl, D. Schaft, A. Roguev, M. Pamblanco et al., 2006   Protein interactions within the Set1 complex and their roles in the regulation of histone 3 lysine 4 methylation. J. Biol. Chem. 281(46): 35404–35412. https://doi.org/10.1074/jbc.M603099200

Dey, B. K., L. Stalker, A. Schnerch, M. Bhatia, J. Taylor-Papidimitriou et al., 2008   The histone demethylase KDM5b/JARID1b plays a role in cell fate decisions by blocking terminal differentiation. Mol. Cell. Biol. 28(17): 5312–5327. https://doi.org/10.1128/MCB.00128-08

Duina, A. A., 2011   Histone Chaperones Spt6 and FACT: Similarities and Differences in Modes of Action at Transcribed Genes. Genet. Res. Int. 2011: 625210. https://doi.org/10.4061/2011/625210

Formosa, T., P. Eriksson, J. Wittmeyer, J. Ginn, Y. Yu et al., 2001   Spt16-Pob3 and the HMG protein Nhp6 combine to form the nucleosome-binding factor SPN. EMBO J. 20(13): 3506–3517. https://doi.org/10.1093/emboj/20.13.3506

Hainer, S. J., J. A. Pruneski, R. D. Mitchell, R. M. Monteverde, and J. A. Martens, 2011   Intergenic transcription causes repression by directing nucleosome assembly. Genes Dev. 25(1): 29–40. https://doi.org/10.1101/gad.1975011

Ingvarsdottir, K., C. Edwards, M. G. Lee, J. S. Lee, D. C. Schultz et al., 2007   Histone H3 K4 demethylation during activation and attenuation of GAL1 transcription in Saccharomyces cerevisiae. Mol. Cell. Biol. 27(22): 7856–7864. https://doi.org/10.1128/MCB.00801-07

Ivanovska, I., P. E. Jacques, O. J. Rando, F. Robert, and F. Winston, 2011   Control of chromatin structure by spt6: different consequences in coding and regulatory regions. Mol. Cell. Biol. 31(3): 531–541. https://doi.org/10.1128/MCB.01068-10

Kaplan, C. D., L. Laprade, and F. Winston, 2003   Transcription elongation factors repress transcription initiation from cryptic sites. Science 301(5636): 1096–1099. https://doi.org/10.1126/science.1087374

Kim, T., and S. Buratowski, 2009   Dimethylation of H3K4 by Set1 recruits the Set3 histone deacetylase complex to 5′ transcribed regions. Cell 137(2): 259–272. https://doi.org/10.1016/j.cell.2009.02.045

Krogan, N. J., J. Dover, S. Khorrami, J. F. Greenblatt, J. Schneider et al., 2002   COMPASS, a histone H3 (Lysine 4) methyltransferase required for telomeric silencing of gene expression. J. Biol. Chem. 277(13): 10753–10755. https://doi.org/10.1074/jbc.C200023200

Lenstra, T. L., J. J. Benschop, T. Kim, J. M. Schulze, N. A. Brabers et al., 2011   The specificity and topology of chromatin interaction pathways in yeast. Mol. Cell 42(4): 536–549. https://doi.org/10.1016/j.molcel.2011.03.026

Li, Z., F. J. Vizeacoumar, S. Bahr, J. Li, J. Warringer et al., 2011   Systematic exploration of essential yeast gene function with temperature-sensitive mutants. Nat. Biotechnol. 29(4): 361–367. https://doi.org/10.1038/nbt.1832

Liang, G., R. J. Klose, K. E. Gardner, and Y. Zhang, 2007   Yeast Jhd2p is a histone H3 Lys4 trimethyl demethylase. Nat. Struct. Mol. Biol. 14(3): 243–245 (erratum: Nat. Struct. Mol. Biol. 14: 351). https://doi.org/10.1038/nsmb1204

Lopez-Bigas, N., T. A. Kisiel, D. C. Dewaal, K. B. Holmes, T. L. Volkert et al., 2008   Genome-wide analysis of the H3K4 histone demethylase RBP2 reveals a transcriptional program controlling differentiation. Mol. Cell 31(4): 520–530. https://doi.org/10.1016/j.molcel.2008.08.004

Lorenz, D. R., L. F. Meyer, P. J. Grady, M. M. Meyer, and H. P. Cam, 2014   Heterochromatin assembly and transcriptome repression by Set1 in coordination with a class II histone deacetylase. eLife 3: e04506. https://doi.org/10.7554/eLife.04506

Ma, Z., D. Atencio, C. Barnes, H. DeFiglio, and S. D. Hanes, 2012   Multiple roles for the Ess1 prolyl isomerase in the RNA polymerase II transcription cycle. Mol. Cell. Biol. 32(17): 3594–3607. https://doi.org/10.1128/MCB.00672-12

Margaritis, T., V. Oreal, N. Brabers, L. Maestroni, A. Vitaliano-Prunier et al., 2012   Two distinct repressive mechanisms for histone 3 lysine 4 methylation through promoting 3′-end antisense transcription. PLoS Genet. 8(9): e1002952. https://doi.org/10.1371/journal.pgen.1002952

Martens, J. A., L. Laprade, and F. Winston, 2004   Intergenic transcription is required to repress the Saccharomyces cerevisiae SER3 gene. Nature 429(6991): 571–574. https://doi.org/10.1038/nature02538

Martens, J. A., P. Y. Wu, and F. Winston, 2005   Regulation of an intergenic transcript controls adjacent gene transcription in Saccharomyces cerevisiae. Genes Dev. 19(22): 2695–2704. https://doi.org/10.1101/gad.1367605

McCullough, L., Z. Connell, C. Petersen, and T. Formosa, 2015   The Abundant Histone Chaperones Spt6 and FACT Collaborate to Assemble, Inspect, and Maintain Chromatin Structure in Saccharomyces cerevisiae. Genetics 201(3): 1031–1045. https://doi.org/10.1534/genetics.115.180794

McDonald, S. M., D. Close, H. Xin, T. Formosa, and C. P. Hill, 2010   Structure and biological importance of the Spn1-Spt6 interaction, and its regulatory role in nucleosome binding. Mol. Cell 40(5): 725–735. https://doi.org/10.1016/j.molcel.2010.11.014

Mersman, D. P., H. N. Du, I. M. Fingerman, P. F. South, and S. D. Briggs, 2009   Polyubiquitination of the demethylase Jhd2 controls histone methylation and gene expression. Genes Dev. 23(8): 951–962. https://doi.org/10.1101/gad.1769209

Mikheyeva, I. V., P. J. Grady, F. B. Tamburini, D. R. Lorenz, and H. P. Cam, 2014   Multifaceted genome control by Set1 Dependent and Independent of H3K4 methylation and the Set1C/COMPASS complex. PLoS Genet. 10(10): e1004740. https://doi.org/10.1371/journal.pgen.1004740

Nagy, P. L., J. Griesenbeck, R. D. Kornberg, and M. L. Cleary, 2002   A trithorax-group complex purified from Saccharomyces cerevisiae is required for methylation of histone H3. Proc. Natl. Acad. Sci. USA 99(1): 90–94. https://doi.org/10.1073/pnas.221596698

Nedea, E., X. He, M. Kim, J. Pootoolal, G. Zhong *et al.*, 2003   Organization and function of APT, a subcomplex of the yeast cleavage and polyadenylation factor involved in the formation of mRNA and small nucleolar RNA 3′-ends. J. Biol. Chem. 278: 33000–33010.

O'Donnell, A. F., N. K. Brewster, J. Kurniawan, L. V. Minard, G. C. Johnston *et al.*, 2004   Domain organization of the yeast histone chaperone FACT: the conserved N-terminal domain of FACT subunit Spt16 mediates recovery from replication stress. Nucleic Acids Res. 32(19): 5894–5906. https://doi.org/10.1093/nar/gkh922

Orphanides, G., G. LeRoy, C. H. Chang, D. S. Luse, and D. Reinberg, 1998   FACT, a factor that facilitates transcript elongation through nucleosomes. Cell 92(1): 105–116. https://doi.org/10.1016/S0092-8674(00)80903-4

Orphanides, G., W. H. Wu, W. S. Lane, M. Hampsey, and D. Reinberg, 1999   The chromatin-specific transcription elongation factor FACT comprises human SPT16 and SSRP1 proteins. Nature 400(6741): 284–288. https://doi.org/10.1038/22350

Porrua, O., and D. Libri, 2013   A bacterial-like mechanism for transcription termination by the Sen1p helicase in budding yeast. Nat. Struct. Mol. Biol. 20(7): 884–891. https://doi.org/10.1038/nsmb.2592

Pruneski, J. A., and J. A. Martens, 2011   Transcription of intergenic DNA deposits nucleosomes on promoter to silence gene expression. Cell Cycle 10(7): 1021–1022. https://doi.org/10.4161/cc.10.7.15167

Ramakrishnan, S., S. Pokhrel, S. Palani, C. Pflueger, T. J. Parnell *et al.*, 2016   Counteracting H3K4 methylation modulators Set1 and Jhd2 co-regulate chromatin dynamics and gene transcription. Nat. Commun. 7: 11949. https://doi.org/10.1038/ncomms11949

Santos-Rosa, H., R. Schneider, B. E. Bernstein, N. Karabetsou, A. Morillon *et al.*, 2003   Methylation of histone H3 K4 mediates association of the Isw1p ATPase with chromatin. Mol. Cell 12(5): 1325–1332. https://doi.org/10.1016/S1097-2765(03)00438-6

Sayou, C., G. Millan-Zambrano, H. Santos-Rosa, E. Petfalski, S. Robson *et al.*, 2017   RNA binding by histone methyltransferases Set1 and Set2. Mol. Cell. Biol. 37: e00165-17.

Schibler, A., E. Koutelou, J. Tomida, M. Wilson-Pham, L. Wang *et al.*, 2016   Histone H3K4 methylation regulates deactivation of the spindle assembly checkpoint through direct binding of Mad2. Genes Dev. 30: 1187–1197. https://doi.org/10.1101/gad.278887.116

Schneider, J., A. Wood, J. S. Lee, R. Schuster, J. Dueker *et al.*, 2005   Molecular regulation of histone H3 trimethylation by COMPASS and the regulation of gene expression. Mol. Cell 19(6): 849–856. https://doi.org/10.1016/j.molcel.2005.07.024

Soares, L. M., and S. Buratowski, 2012   Yeast Swd2 is essential because of antagonism between Set1 histone methyltransferase complex and APT (associated with Pta1) termination factor. J Biol Chem 287: 15219–15231.

Soares, L. M., M. Radman-Livaja, S. G. Lin, O. J. Rando, and S. Buratowski, 2014   Feedback control of Set1 protein levels is important for proper H3K4 methylation patterns. Cell Reports 6(6): 961–972. https://doi.org/10.1016/j.celrep.2014.02.017

Soloveychik, M., M. Xu, O. Zaslaver, K. Lee, A. Narula *et al.*, 2016   Mitochondrial control through nutritionally regulated global histone H3 lysine-4 demethylation. Sci. Rep. 6(1): 37942. https://doi.org/10.1038/srep37942

Steinmetz, E. J., and D. A. Brow, 1996   Repression of gene expression by an exogenous sequence element acting in concert with a heterogeneous nuclear ribonucleoprotein-like protein, Nrd1, and the putative helicase Sen1. Mol. Cell. Biol. 16(12): 6993–7003. https://doi.org/10.1128/MCB.16.12.6993

Steinmetz, E. J., N. K. Conrad, D. A. Brow, and J. L. Corden, 2001   RNA-binding protein Nrd1 directs poly(A)-independent 3′-end formation of RNA polymerase II transcripts. Nature 413(6853): 327–331. https://doi.org/10.1038/35095090

Takahashi, Y. H., J. S. Lee, S. K. Swanson, A. Saraf, L. Florens *et al.*, 2009   Regulation of H3K4 trimethylation via Cps40 (Spp1) of COMPASS is monoubiquitination independent: implication for a Phe/Tyr switch by the catalytic domain of Set1. Mol. Cell. Biol. 29(13): 3478–3486. https://doi.org/10.1128/MCB.00013-09

Taverna, S. D., S. Ilin, R. S. Rogers, J. C. Tanny, H. Lavender *et al.*, 2006   Yng1 PHD finger binding to H3 trimethylated at K4 promotes NuA3 HAT activity at K14 of H3 and transcription at a subset of targeted ORFs. Mol. Cell 24(5): 785–796. https://doi.org/10.1016/j.molcel.2006.10.026

Terzi, N., L. S. Churchman, L. Vasiljeva, J. Weissman, and S. Buratowski, 2011   H3K4 trimethylation by Set1 promotes efficient termination by the Nrd1-Nab3-Sen1 pathway. Mol. Cell. Biol. 31(17): 3569–3583. https://doi.org/10.1128/MCB.05590-11

Thiebaut, M., E. Kisseleva-Romanova, M. Rougemaille, J. Boulay, and D. Libri, 2006   Transcription termination and nuclear degradation of cryptic unstable transcripts: a role for the nrd1-nab3 pathway in genome surveillance. Mol. Cell 23(6): 853–864. https://doi.org/10.1016/j.molcel.2006.07.029

Tokai, M., H. Kawasaki, Y. Kikuchi, and K. Ouchi, 2000   Cloning and characterization of the CSF1 gene of Saccharomyces cerevisiae, which is required for nutrient uptake at low temperature. J. Bacteriol. 182(10): 2865–2868. https://doi.org/10.1128/JB.182.10.2865-2868.2000

Trésaugues, L., P. M. Dehé, R. Guérois, A. Rodriguez-Gil, I. Varlet *et al.*, 2006   Structural characterization of Set1 RNA recognition motifs and their role in histone H3 lysine 4 methylation. J. Mol. Biol. 359(5): 1170–1181. https://doi.org/10.1016/j.jmb.2006.04.050

Ursic, D., K. L. Himmel, K. A. Gurley, F. Webb, and M. R. Culbertson, 1997   The yeast SEN1 gene is required for the processing of diverse RNA classes. Nucleic Acids Res. 25(23): 4778–4785. https://doi.org/10.1093/nar/25.23.4778

Vanacova, S., and R. Stefl, 2007   The exosome and RNA quality control in the nucleus. EMBO Rep. 8(7): 651–657. https://doi.org/10.1038/sj.embor.7401005

Vasiljeva, L., and S. Buratowski, 2006   Nrd1 interacts with the nuclear exosome for 3′ processing of RNA polymerase II transcripts. Mol. Cell 21(2): 239–248. https://doi.org/10.1016/j.molcel.2005.11.028

Xu, M., M. Soloveychik, M. Ranger, M. Schertzberg, Z. Shah *et al.*, 2012   Timing of transcriptional quiescence during gametogenesis is controlled by global histone H3K4 demethylation. Dev. Cell 23(5): 1059–1071. https://doi.org/10.1016/j.devcel.2012.10.005

Zhang, K., W. Lin, J. A. Latham, G. M. Riefler, J. M. Schumacher *et al.*, 2005   The Set1 methyltransferase opposes Ipl1 aurora kinase functions in chromosome segregation. Cell 122(5): 723–734. https://doi.org/10.1016/j.cell.2005.06.021

Communicating editor: N. Rhind